ACS OMEGA

http://pubs.acs.org/journal/acsodf

Article

Transesterification of *Camelina sativa* Oil Catalyzed by Mg/Al Mixed Oxides with Added Divalent Metals

Miroslava Mališová, Michal Horňáček, Jozef Mikulec, Pavol Hudec, Martin Hájek, András Peller, Vladimír Jorík, Karel Frolich, Marcela Hadvinová, and Elena Hájeková*

Cite This: *ACS Omega* 2020, 5, 32040–32050

Read Online

ACCESS | Metrics & More | Article Recommendations | Supporting Information

ABSTRACT: This paper is focused on the heterogeneously catalyzed transesterification (in a batch reactor) of vegetable oil, including the determination of leached metals. The oil was obtained from the short-season crop *Camelina sativa*. The reaction was catalyzed by mixed oxides, which were synthesized from Mg/Al hydrotalcites with built-in different types of divalent cations such as Mn, Ca, Co, Ni, and Fe. The various physicochemical properties like the structure by X-ray diffraction, acidity, basicity, and textural properties were measured and the effect of the added cation type on catalyst properties and activity was compared. A noticeable relationship between the cation type and catalytic activity in the transesterification reaction was observed. The highest ester content of 96.6 wt % after 7 h of transesterification was observed for catalysts with nickel and iron. The statistical analysis of results showed that the catalyst activity was mainly influenced by middle-temperature basic sites. The novelty lies in transesterification over five different heterogeneous catalysts—mixed oxides with added divalent metals at the same reaction conditions of *C. sativa* oil.

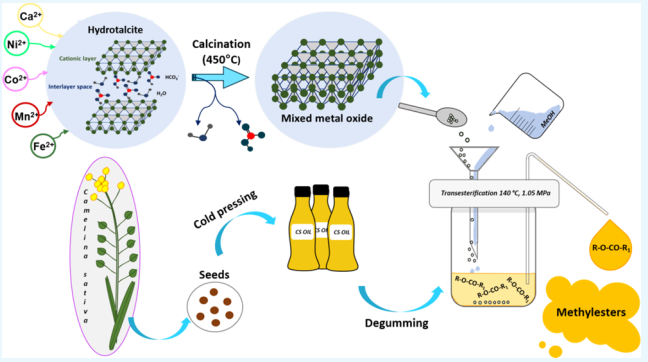

1. INTRODUCTION

With the increase in the population, as well as transport and car needs, the production of a sufficient amount of good-quality fuels is a challenge. Alternative fuels were examined long before the significant increase in population and petroleum consumption started. The first idea for using vegetable oil as fuel in engines was presented in 1900 at the Paris World Exposition. Rudolf Diesel made this idea real when he used peanut oil as a fuel in his design of the diesel engine.[1]

Camelina sativa (L.) Crantz (CS) represents an alternative oil-seed crop. CS offers many advantages for biofuel production. It is a flexible plant and can grow under different climatic conditions as an annual summer crop or biannual winter crop. CS is not demanding with regard to soil quality and is relatively resistant to drought in comparison with commonly used rapeseed. It can also grow on contaminated soils. The content of oil in summer varieties of the seed is about 42% on a dry matter basis, while in winter varieties, it is about 45%.[2] Oil from CS offers a high content of tocopherols (700 mg/kg) and phenolic compounds (128 mg/kg as chlorogenic acid), which makes oil from CS more stable toward oxidation.[3] The main disadvantage of CS oil as a source for biodiesel production is the high content of polyunsaturated fatty acids, which results in a higher iodine number of methyl esters (MEs) than is the standard value (EN 14103) for biodiesel.[4]

Transesterification of vegetable oils containing triglycerides with alcohol under basic or acid conditions produces fatty acid alkyl esters and glycerol.[5] For the base homogeneous-catalyzed transesterification, the KOH, NaOH, and sodium methoxide catalysts are commonly used for biodiesel preparation. The process of homogenous transesterification proceeds under mild reaction conditions with a short reaction time and high yields of fatty acid methyl ester (FAME) (around 99 wt %).[6] However, every process has its drawbacks. It is quite difficult to separate liquid products and homogeneous catalysts, which is easier in the case of heterogeneous transesterification.[7] In basic homogeneous transesterification, emulsification is another complication, while the use of a solid catalyst eliminates this problem.[8] Another advantage of heterogeneous transesterification is the smaller catalyst demand per reaction.[9] According to Zhang et al., the catalyst consumption of NaOH is 88 tonnes for 8000 tonnes of biodiesel.[10] In the case of MgO, only

Received: October 12, 2020
Accepted: November 20, 2020
Published: December 4, 2020

https://dx.doi.org/10.1021/acsomega.0c04976
ACS Omega 2020, 5, 32040–32050

5.7 tonnes of this solid catalyst is necessary for the production of 100 000 tonnes of biodiesel.[9] The most important advantage of heterogeneous transesterification is the possibility of catalyst regeneration and reuse. One of the perspective heterogeneous catalysts is the mixed oxides (MO) obtained from hydrotalcites (HT).

Hydrotalcites, also known as layered double hydroxides, can be used as materials for the preparation of mixed oxides by calcination around the temperature of 400−500 °C because of their easy preparation by coprecipitation.[11] Mixed oxides exhibit a high specific surface area and a high content of basic sites, which is important for their catalytic activity.[12] For this reason, they are widely studied as basic heterogeneous catalysts for biodiesel preparation via transesterification. Basic hydrotalcite contains Al^{3+} and Mg^{2+} cations in their cationic layers, but many other cations can also be incorporated;[13,14] hence, the catalytic properties of the prepared mixed oxides are changed. The divalent and trivalent cations are most commonly used for mixed oxide preparation because of their possibility to replace Mg^{2+} or Al^{3+} cations in the octahedral structure of hydrotalcite.[15] Several authors studied the relationship between different cations incorporated into the structure and their catalytic activity. Wang et al.[16] observed that the Fe^{2+} cation can substitute for the Mg^{2+} position, causing higher basicity and conversion into FAME. Based on the study of Wang et al.,[17] mixed oxides with Ni^{2+} built into the structure cause high FAME yields and easy separation of the catalyst from methyl esters in comparison to the sample without Ni.

Preparation ways and preparation conditions of hydrotalcite synthesis, together with the characterization of their properties, was the field of our research in the preliminary study. The novelty of the present research lies in the building of five different divalent cations into the structure of mixed oxide and the observation of the relationship between the cation type and structural properties or catalytic activity of the prepared mixed oxides in the transesterification of alternative *C. sativa* vegetable oil. CS oil as a source for biodiesel was used by other researchers, but mostly in homogeneous transesterification. Heterogeneous transesterification, as a possible way of biodiesel preparation, was tested only by a few authors.[18−20] In the present research, a heterogeneous way was successfully applied. Reaction conditions such as temperature, the amount of catalyst, and the molar ratio of methanol/oil were chosen based on the results of our previous research.

2. RESULTS AND DISCUSSION

2.1. Catalyst Characterization. *2.1.1. Metal Content in Prepared Hydrotalcites.* Five hydrotalcites, with different divalent cation built-in structures, were prepared. As shown in Table 1, where all prepared hydrotalcites are listed, the metal content in all prepared hydrotalcites is almost the same. The molar ratio of metals in the prepared HT was similar to the theoretical content calculated from the prepared solutions.

Table 1. List of Prepared Hydrotalcites (HT) and Their Metal Contents (X = Added Metal)

hydrotalcites	w_{Mg}, wt %	w_{Al}, wt %	w_X, wt %	molar ratio Mg/Al/X	molar ratio M^{2+}/M^{3+}
Ni/HT	16.3	10.8	9.5	4.1/2.5/1	2/1
Mn/HT	15.3	10.5	8.4	4.1/2.4/1	2/1
Ca/HT	15.6	10.2	6.2	4.1/2.4/1	2/1
Co/HT	15.3	10.6	9.5	3.9/2.4/1	2/1
Fe/HT	15.5	10.3	8.8	4/2.4/1	2/1

2.1.2. X-ray Diffraction (XRD). The diffractograms of hydrotalcites (HT) and mixed oxides (MO) are shown in Figure 1A,B. For hydrotalcites, the intense diffraction lines were observed at 12, 28, 41, 55, and 72°. These lines are typical for hydrotalcite structures of rhombohedral symmetry.[21] The peak at around 12° 2θ is attributed to planes (110) and a peak at 72° 2θ to planes (006). These reflections were used to calculate the basal spacing (d_{003}, d_{110}) between cation layers (Table 2). The differences between d parameters are negligible. Spacings of crystallographic planes (110) and (006) were used for the calculation of the lattice parameter (a and c). Parameter a, calculated as $a = 2{\cdot}d_{110}$, represents the average distance between cation−cation (metal−metal) in the cationic layer of the hydrotalcite structure, also known as unit cell dimension.[22] The second crystallographic parameter c, calculated as $c = 3{\cdot}d_{110}$, represents the thickness of one brucite-like layer and interlayer.[23] A significant impact of a cation type on a lattice parameter was not observed. Based on the results shown in Table 2, the crystallite size in the samples is different. A significantly smaller crystallite size in the case of sample Ni/HT was observed. Hernández et al.,[24] as well as Silva et al.,[22] attributed larger crystallite size to different contents of metal cations in the structure, which indicates the impact of the cation type on the hydrotalcite structure.

On diffractograms of MO (Figure 2B), typical lines were observed, which confirms mixed oxide structure formation by calcination of hydrotalcites. The lower intensity of reflections in comparison with hydrotalcite diffractograms indicates the amorphous structure, which is characteristic of mixed oxides.

2.1.3. Thermogravimetry (TG). The reasons for thermogravimetry analysis (TGA) are (i) the selection of suitable calcination temperature and (ii) the monitoring of the influence of added metal on the weight loss (WL), the temperature of dehydration, and the decomposition of individual hydrotalcite (Table 3).

First, a slight decrease in weight was observed from the temperature of about 40 °C, which corresponds to the removal of physisorbed water from the surface of hydrotalcite. Based on the study of Wang et al., the physisorbed water molecules are removed until the temperature reaches 100 °C.[16] The two significant weight losses were observed during the next temperature increase. The first decrease (Table 3) at around 180−200 °C is ascribed to dehydration, i.e., the removal of water from the interlayer space. Wang et al. attributed this loss to the removal of chemically adsorbed water from the internal and external surface of hydrotalcite.[16] The weight loss at around 15 wt % during dehydration steps indicates the amount of water in the interlayer space. The different binding force of water molecules in the interlayer space is reflected in the differences between temperatures of the first decrease. The second intense weight loss around temperatures of 320−420 °C (Table 3) belongs to the combination of decomposition (HCO_3^- is removed from the interlayer space) and dehydroxylation (the elimination of OH^- anions from the hydrotalcite structure). At this temperature, the hydrotalcite-layered structure collapsed and passed to the structure of mixed oxides. The obtained results confirm that all hydrotalcite samples converted into mixed oxide up to 450 °C, which was the calcination temperature used in this work. Curves obtained

https://dx.doi.org/10.1021/acsomega.0c04976
ACS Omega 2020, 5, 32040−32050

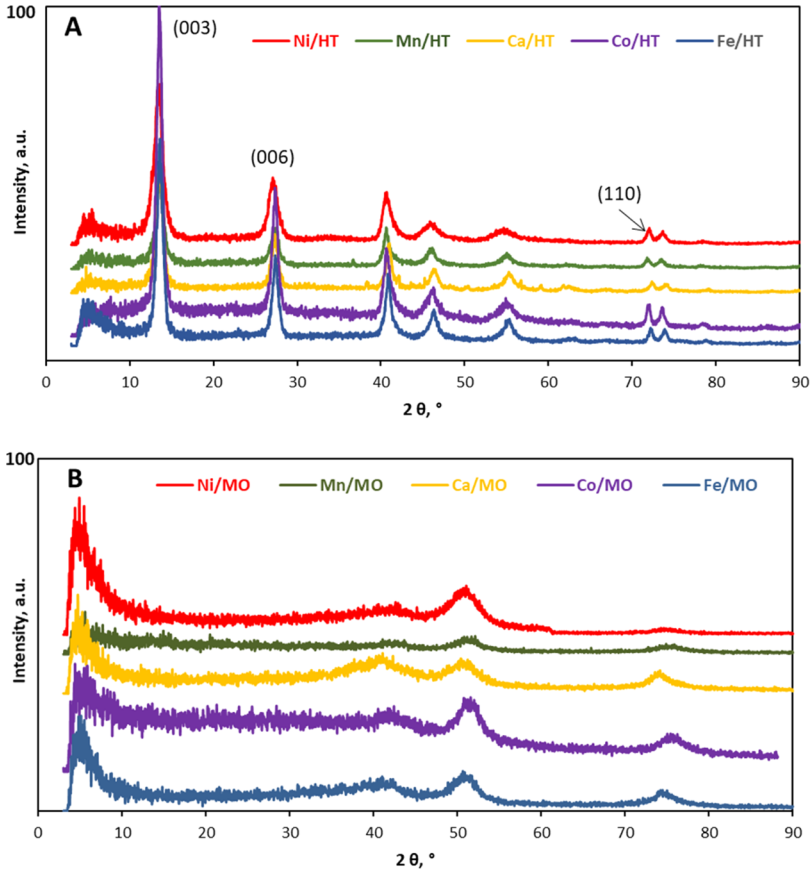

Figure 1. XRD pattern of hydrotalcite (A) and mixed oxides (B).

Table 2. Parameters Calculated from XRD Pattern of Hydrotalcite

hydrotalcites	d_{003}, Å	d_{110}, Å	D, nm	a, Å	c, Å
Ni/HT	7.67	1.54	7.80	3.08	22.99
Mn/HT	7.56	1.53	11.42	3.06	22.69
Ca/HT	7.55	1.52	11.17	3.03	22.64
Co/HT	7.60	1.52	13.40	3.05	22.79
Fe/HT	7.56	1.52	11.81	3.03	22.69

by thermogravimetry and derivated thermogravimetry of all materials were similar.

The total weight loss of all samples is around 40 wt %, which means that around 40 wt % of hydrotalcite mass is made of anions and water molecules in interlayer space.

2.1.4. Textural Properties. The specific surface area of all mixed oxides obtained from hydrotalcite by calcination at 450 °C was measured. As shown in Table 4, the Ni/MO achieved the highest value (262 m^2/g). The mixed oxides with additional metals Mn and Fe showed lower surface areas. The specific surface area is an important parameter of a heterogeneous catalyst. The amount and availability of catalytic active sites of the surface increase with the increase of the specific surface area. The pore volume is another important parameter along with the specific surface area. Differences between the pore volumes are significant. Mixed oxide with Ca built into the structure achieved the lowest pore volume (0.428 cm^3/g), while Fe/MO reached the highest value V_p (0.818 cm^3/g). Wei et al.[25] observed similar results of textural properties for mixed oxide with Ni, where the value of S_{BET} reached 287 m^2/g and V_p 0.63 cm^3/g. Jiang et al.[26] detected a lower value of the specific surface area S_{BET} 158 m^2/g of mixed oxide with Co, in comparison with Co/MO (180 m^2/g) (Table 4). A more significant difference between our results and those of Jiang et al.[26] is in the case of pore volume, where Jiang et al. reached V_p just 0.44 cm^3/g, while Co/MO reached almost 2 times higher value (Table 4). Castro et al.[27] measured the specific surface area for samples of mixed oxides with Ca built in the structure with different Ca contents. The sample with the least content of Ca reached just 82 m^2/g. With the increasing Ca content, the S_{BET} value decreased. In comparison with this, Ca/MO in this work reached even 147 m^2/g (Table 4).

The pore diameter (D_p) is also an important catalyst property. The reached values of D_p for all mixed oxides belong to mesopores (5−47 nm). The widest pore size distribution was observed for Ca/MO; on the other hand, the Ni/MO reached the narrowest distribution (Table 4).

2.1.5. Basicity and Acidity of the Catalyst. The transesterification catalyzed by mixed oxides occurs by a basic mechanism. The basicity of all samples of mixed oxides was measured (Table 5). The basicity of the measured mixed oxides varies from 0.292 to 0.541 mmol CO_2/g. The Ni/MO contains the highest number of basic sites. The Mn/MO and Ca/MO also show a high concentration of basic sites. The mixed oxide with Co built into the structure contains the lowest number of basic sites. The relationship between the type of metal built into the mixed oxide and between the content of basic sites is significant. Not just the final number of basic sites but also the desorption curve of CO_2 indicates catalyst activity. Basic sites can be divided based on desorption temperature. Different scientists use various boundary temper-

https://dx.doi.org/10.1021/acsomega.0c04976
ACS Omega 2020, 5, 32040−32050

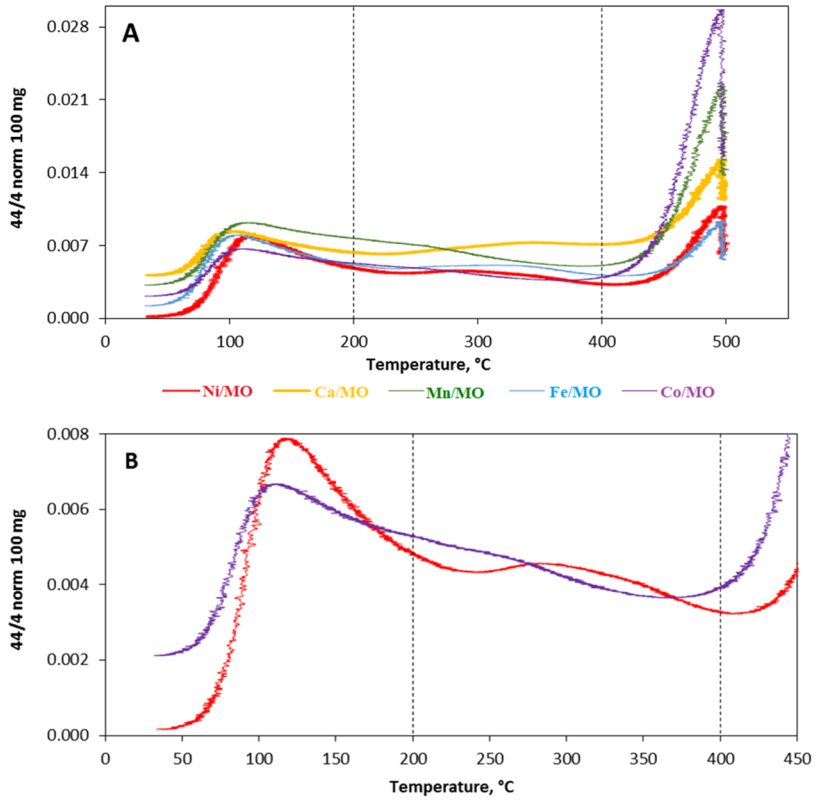

Figure 2. Temperature-programmed desorption of carbon dioxide (TPD-CO_2) profiles of all mixed oxides (A) and comparison of Ni/MO and Co/MO (B).

Table 3. Recorded Temperatures, Weight Losses (WL), and Total Weight Losses (TWL) of Hydrotalcite from TG Analysis

	dehydration		decomposition		
hydrotalcites	T_1, °C	WL_1, wt %	T_2, °C	WL_2, wt %	TWL, wt %
Ni/HT	200	14.8	345	18.1	43.6
Mn/HT	185	12.9	331	19.6	40.9
Ca/HT	175	11.3	359	20.6	39.9
Co/HT	180	12.1	342	19.3	41.2
Fe/HT	178	13.9	369	18.2	42.2

Table 4. Textural Properties of Mixed Metal Oxides

mixed oxides	S_{BET}, m^2/g	V_p, cm^3/g	D_p, nm
Ni/MO	262	0.632	5−19
Mn/MO	220	0.783	19−43
Ca/MO	147	0.428	13−47
Co/MO	180	0.710	16−39
Fe/MO	200	0.818	16−44

atures for each group of sites. Figure 2 represents the division based on the study of Martins et al.[28] Martins et al.[28] divided the desorption curve into three parts. First is the location of weak basic sites, starting from zero temperature to 200 °C. These sites are represented by a peak around the temperature of 100 °C. Di Serio et al.[29] attributed this area to physisorbed CO_2 molecules. The second part, between 200 and 400 °C, based on the study of Martins et al.,[28] belongs to moderate basic sites. Some authors, such as Hernández et al.,[24] divide desorption curves in different ways. In their work, the part over 200 °C belongs to strong basic sites related to the desorption of CO_2 bonded with low coordination O_2^-, while Martins et al.[28] located strong basic sites over 400 °C. Di Serio et al.[29] ascribed the peak located in the moderate basic sites at temperature starting from 350 °C to superbasicity. Figure 2 represents division based on the study of Martins et al.[28]

The acidity of all samples of mixed oxides was also measured. The value of acidity was not higher than 0.8 mmol NH_3/g. The sample Co/MO achieved the highest value of acidity.

Table 5. Basicity Curve Division, Acidity, and Total Basicity of Mixed Metal Oxides

mixed oxides	low t.a.[a], area %	middle t.a.[a], area %	high t.a.[a], area %	total basicity, mmol CO_2/g	acidity, mmol/g
Ni/MO	37	39	24	0.541	0.56
Mn/MO	35	33	31	0.406	0.66
Ca/MO	29	36	35	0.317	0.62
Co/MO	26	24	50	0.292	0.75
Fe/MO	39	39	23	0.497	0.41

[a]Low-temperature area (0−200 °C), middle-temperature area (200−400 °C), high-temperature area (400 °C>).

https://dx.doi.org/10.1021/acsomega.0c04976
ACS Omega 2020, 5, 32040−32050

Table 6. Methyl Ester (ME) Content, Yield, Amount of Leached Metals, and Acid Number of Products after 7 h of Transesterification

mixed oxides	ME content, wt %	ME yield, wt %	Mg, mg/kg	Al, mg/kg	X, mg/kg	acid number, mg KOH/g
Ni/MO	96.7	89.9	1.6	1.1	1.9	0.16
Mn/MO	87.1	78.7	28.5	20.7	11.0	0.18
Ca/MO	92.2	79.7	1.0	3.5	13.5	0.15
Co/MO	77.1	71.9	32.7	25.3	13.7	0.17
Fe/MO	96.6	90.1	47.9	17.5	0.2	0.20

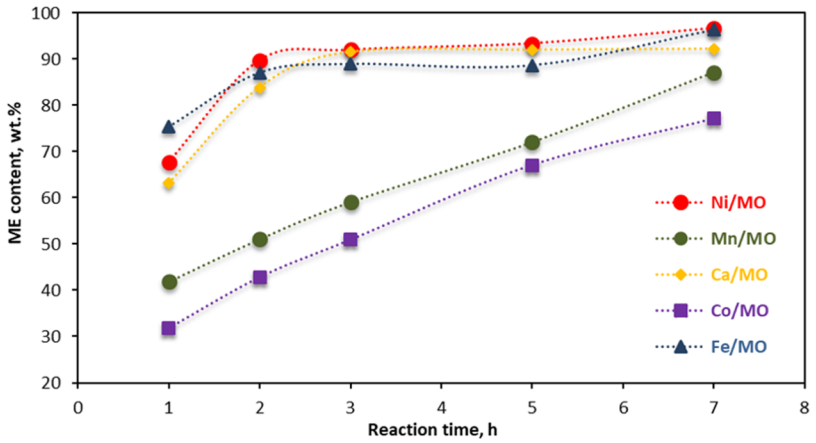

Figure 3. Dependence of the methyl ester (ME) content on reaction time.

2.2. Transesterification of Camelina Oil. The content of methyl esters in the product after heterogeneous transesterification was chosen as the main parameter for the assessment of the transesterification reaction (Table 6). According to standard EN 14214 for biodiesel quality, the minimal value of the methyl ester content is 96.5 wt %. The catalyst containing nickel achieved the highest content of methyl esters after 7 h of transesterification. This was followed by the catalyst Fe/MO with a comparatively high methyl ester content. These two catalysts, unlike mixed oxides with Ca, Mn, and Co metals, accomplish, in the ester phase (EP), minimal methyl ester content given by the standard method for biodiesel quality. The lowest methyl ester content was achieved in the presence of Co/MO. Based on the results of transesterification, each metal added to the structure significantly influenced the structure of hydrotalcite and mixed oxide and associated catalyst activity during the reaction. Wang et al.,[17] in a study of soybean oil transesterification at 65 °C, concluded that mixed oxides with nickel in their structure reached after 6 h of transesterification a conversion of FAME up to 87%, while basic Mg/Al mixed oxide reached lower conversion of around 60%. These results indicate the positive impact of added nickel on catalyst activity. The Fe/MO was another successful catalyst in transesterification with the ME content greater than 96.5 wt % (Table 6). Also, Macala et al.[30] compared hydrotalcites prepared by coprecipitation with Fe built into the structure of basic Mg/Al hydrotalcites in transesterification. The results showed that the catalyst with added Fe reached a higher specific surface area in comparison to basic Mg/Al. Also, oil conversion after 60 min of transesterification at 60 °C was 4 times higher over mixed oxide with Fe in comparison to an undoped Mg/Al catalyst. The results from the comparison of different added amounts of iron confirm the significant impact of added metals on catalytic activity. ME yields obtained after 7 h of transesterification are shown in Table 6, and they varied from 71.9% (Co/MO) to 90.1% (Fe/MO).

There are only some authors who studied heterogeneous transesterification of *C. sativa* oil. Patil et al.[19] used different oxides (BaO, CaO, MgO, SrO) for transesterification. The oxides of barium and strontium yielded 80 wt % of ME after 3 h of transesterification at a temperature of 130 °C. The limitation of this catalytic system is its toxicity and noxious properties. Oxides of Mg and Ca yielded only around 30 wt % of ME after 3 h at different conditions.[31] In comparison with these results, each of the mixed oxides used in our study after 3 h of reaction yielded more than 50 wt % of ME in the ester phase.

To compare individual catalyst activity in transesterification, the samples were taken throughout the entire reaction at precisely specified times. The methyl ester content dependent of the reaction time for all catalysts was determined (Figure 3). The significant differences between the catalyst activity in the first 3 h of transesterification were observed. For mixed oxide with manganese and cobalt built into the structure, the reaction start-up was slow and the methyl ester content was below 60% in the third hour of reaction. In comparison to Mn and Co mixed oxides, the samples Ni/MO, Ca/MO, and Fe/MO achieved over 87% methyl ester content in the third hour. Thus, the activity of the catalysts (Co/MO and Mn/MO) was significantly lower. Based on the course of the methyl ester content as a function of reaction time for Co/MO and Mn/MO, it is possible that due to the lower catalyst activity, equilibrium in the system was not achieved, even after 7 h of reaction. In the case of Ni/MO, Ca/MO, and Fe/MO, equilibrium was observed after 3 h of reaction, which is indicated by minimal changes in the methyl ester content during the rest of the reaction. The comparison of the curves shows that the type of added metal of mixed oxides affects the

https://dx.doi.org/10.1021/acsomega.0c04976
ACS Omega 2020, 5, 32040−32050

catalytic activity, especially at the start of the reaction before equilibrium in the system is reached.

2.3. Methyl Ester Quality. The amount of leached metals in the ester phase was measured because of the possible decomposition of the catalyst structure and its stability during the reaction. As shown in Table 6, the smallest amount of metals leached from the sample Ni/MO. In the case of other samples, like Fe/MO or Co/MO, much more metal leached to the ester phase. The obtained results indicate that the structure created during the preparation of the catalyst and the bonding strength between metals in the cationic layer probably varied in samples with different metal cations used for synthesis. As a result, the resistance against metal leaching to the ester phase is different from different catalysts. From this point of view, nickel seems to be the most suitable metal for the addition to hydrotalcites because of the small amount of leached metals in the product and the high content of ME after transesterification.

Representation of ME in the product after 7 h of transesterification over Ni/HT is shown in Table 7. The content of polyunsaturated acids bonded in triglycerides depends on the oil type, and in camelina oil is higher in comparison to the commonly used oil for transesterification, rapeseed oil. The most significant difference lies in the content of polyunsaturated acids (C18:2 and C18:3). Their content in camelina oil is 53.6 wt %, while in rapeseed oil it is around 34 wt %.[32]

Table 7. Representation of Methyl Ester (ME) in the Product after 7 h of Transesterification over Ni/MO

ME			
type	content, wt %	type	content, wt %
C12:0	0.01	C20:1	14.7
C14:0	0.07	C20:2	1.7
C16:0	5.3	C20:3	1.1
C18:0	2.5	C22:0	0.3
C18:1	15.4	C22:1	3.0
C18:2	18.4	C24:0	0.3
C18:3	32.9	C24:1	0.6
C20:0	1.5		

The value of iodine number is associated with the content of unsaturated fatty acid methyl esters and it did not change through the reaction. Iodine number of ME for different used catalysts varied from 150 to 153 g I_2/100 g. As shown in Table 8, the iodine number for CS oil is 153 g I_2/100 g. The standard EN 14214 prescribes the maximal allowed iodine number for FAME after transesterification up to 120 g I_2/100 g. Because of the high iodine number of ME prepared from camelina oil, it is necessary to reduce it in methyl esters for biofuels. There are two ways to solve the problem. The first option is to mix, in small portions, methyl esters prepared from CS oil and methyl esters prepared from oil with a lower iodine number, like rapeseed oil. The second option is to carry out partial hydrogenation of prepared methyl esters and so to reduce the iodine number. Another important property of ME is the water content. In the case of the prepared ME, the water content was in all products under 300 mg/kg. This content meets the maximum value of 500 mg/kg prescribed by EN 14214.

Table 8. Basic Properties of CS Oil

oil property	raw oil	degummed oil
acid number, mg_{KOH}/g	0.86	0.86
iodine number, g I_2/100 g	153	152
density (20 °C), g/dm^3	922.2	922.2
kinematic viscosity (20 °C), mm^2/s	64.9	65.8
P, mg/kg	13.16	<3
Ca, mg/kg	6.19	<1
Mg, mg/kg	2.51	<1
Na, mg/kg	<1	<1
K, mg/kg	2.85	<1
S, mg/kg	13.65	<5
water content, wt %	0.06	0.05

2.4. Impact of Physical−Chemical Properties of Catalysts on Their Activity. The impact of the main catalyst properties such as the specific surface area, pore volume, pore diameter, and basicity on the catalyst activity was studied. Because of the basic nature of the hydrotalcite-like compound, as well as the mixed oxides, basicity is one of the most important properties of the catalyst. The impact of catalyst basicity on its activity was observed for each catalyst. The Ni/MO catalyst achieved one of the highest ME contents (68 wt %) after 1 h of transesterification, together with the highest content of basic sites from all catalysts (0.541 mmol CO_2/g), as can be seen in Table 5. In comparison, sample Fe/MO achieved a slightly higher content of methyl ester after 1 h of reaction (75 wt %), but its basicity was little lower (0.497 mmol CO_2/g). Similar differences can be seen in the case of Mn/MO and Co/MO. Both catalysts achieved the methyl ester content below 45% after 1 h of transesterification, but the basicity of Mn/MO is visibly higher than the basicity of the equally active Co/MO catalyst. The methyl ester content after 7 h of transesterification correlates better with the middle t.a. of basic sites of mixed oxides (Figure 4), and the number of basic sites in this temperature area has a positive impact on catalyst activity. This linear dependency describes differences between catalyst activity caused by the number of middle-temperature basic sites. The catalyst with a higher content of basic sites that occurs in temperatures between 200 and 400 °C based on the study of Martins et al.[28] is more active in transesterification. Mootabadi et al.[32] attributed the activity of their catalyst in the transesterification of palm oil to basic sites. Bancquart et al.[33] concluded that the reaction rate depends not only on the total basicity but also on the distribution of basic

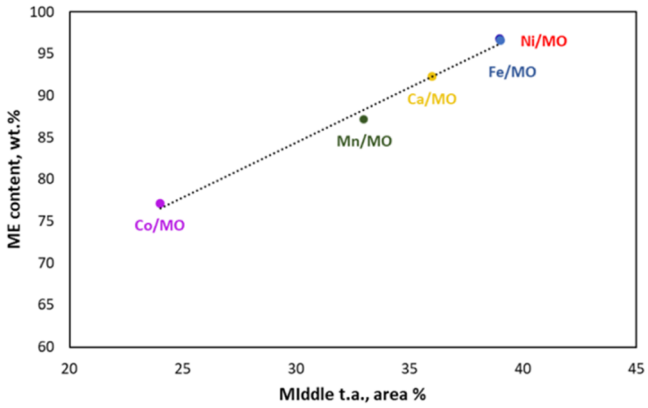

Figure 4. Dependence of the methyl ester (ME) content after 7 h of transesterification on middle t.a. basic sites.

https://dx.doi.org/10.1021/acsomega.0c04976
ACS Omega 2020, 5, 32040−32050

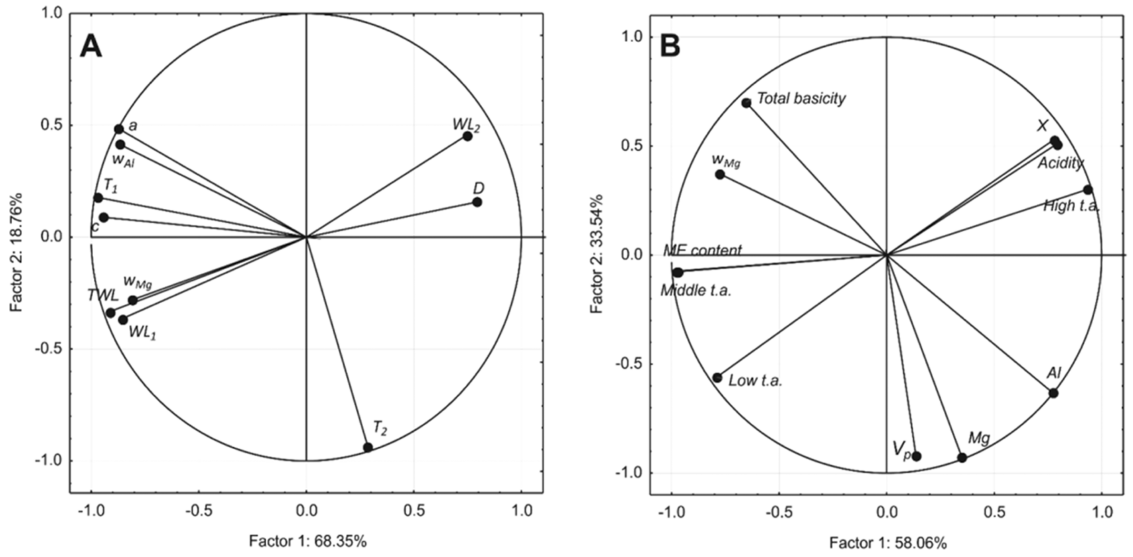

Figure 5. Component weight plot (CWP) for the properties of hydrotalcites (A) and mixed oxides with transesterification results (B).

sites and their strength. Di Serio et al.[29] attributed catalyst activity to superbasic sites, occurring at around a temperature of 300−350 °C. This peak is also visible in Figure 2, in the moderate basic site area. The methyl ester content after 7 h and at the beginning of the reaction confirms that superbasic sites can have the main impact on catalyst activity. While, in the case of the most active sample, Ni/MO shows a visible peak in this area, in the case of the sample Co/MO, one of the least active, there is no presence of a peak in this area and the curve decreases in this place. The same trend was observed in the case of the samples Fe/MO, Ca/MO, and Mn/MO. The relationship between these sites can also indicate the percentage of the area of the middle-temperature peak, which is the highest for Ni/MO and Fe/MO samples.

The number of acidic sites is most commonly measured for acid catalysts. However, the presence of acidic sites can influence the transesterification of vegetable oil because of the simultaneous esterification of free fatty acids (FFA) on the acidic sites. Free fatty acids may react with methanol on the acidic sites to form methyl esters and water. Yan et al.[34] observed simultaneous esterification and transesterification in one step because of the presence of both acidic and basic sites in the catalyst. Transesterification was performed on waste or refined oil with a high content of FFA. Also, Lee et al.[35] described the same conclusions of the possibility of esterification and transesterification of jatropha oil in one step on the catalyst with acidic and basic sites. The amount of FFA in CS oil (0.28 wt %) is relatively small in comparison with other oils such as Jatropha (9 wt %) or waste oil (3.78 wt %). Therefore, the esterification of FFA in CS oil had an insignificant influence on the final methyl ester content in products.

The relationship between textural properties and catalyst activity was also observed. Di Serio et al.[29] concluded that not only basicity affects catalyst activity in the transesterification but also textural properties. As is shown in Table 4, the Ni/MO and the Mn/MO have the highest value of the specific surface area. While the activity of the Ni/MO in the first hour of the reaction is one of the highest, in the case of the Mn/MO, the activity at the beginning of the reaction is one of the lowest. Nevertheless, the specific surface area is an important property for catalyst activity in the transesterification of vegetable oils. An insufficient specific surface area and pore volume, as well as the low content of basic sites, can cause the lowest activity of the catalyst Co/MO. This mixed oxide was the least active from all tested catalysts.

2.5. Statistical Evaluation. The relationship between the dependent variables (the temperature and loss during calcination, the specific surface area, basicity, the ester content, etc.) was analyzed separately for HT and MO (Figure 5A,B). The statistical analysis for all variables together was not carried out because the final graph would be quite confusing.

The properties of mixed oxides are influenced by the properties of hydrotalcites. Therefore, the relationship between the properties of hydrotalcites is also important to describe. For HT, a strong positive correlation was found between the amount of magnesium in HT (w_{Mg}), the weight loss in the first step (water escape, WL_1), and the total weight loss during calcination (TWL), i.e., more magnesium means higher loss during calcination. This can be explained by the fact that water is easily bonded to magnesium compared to other metals in HT. This group (w_{Mg}, WL_1, and TWL) has a negative correlation with temperature in the second step (WL_2) and crystallinity (D), which means that (i) the increase of the magnesium content decreases the crystallinity and (ii) higher weight loss in the first step means lower weight loss in the second step. Another positive correlation was found for the aluminum content in HT and parameter a. The parameter c was positively correlated with the temperature of the first step (T_1) because a higher temperature means more bonded water, which can mean a higher thickness of the interlayer. These first two groups also have a weaker positive correlation with each other. No correlation between the temperature of the second step of the transformation (from TGA) and all other parameters was found.

The most important are correlations between the properties of mixed oxides and transesterification outcomes, i.e., the ME content and metal leaching (Figure 6B). The ME content was strongly positively correlated with the population of the middle basic sites (middle t.a.) and less with the low population of basic sites (low t.a), i.e., the higher the relative population of middle and low basic sites means the higher the ME content.

https://dx.doi.org/10.1021/acsomega.0c04976
ACS Omega 2020, 5, 32040−32050

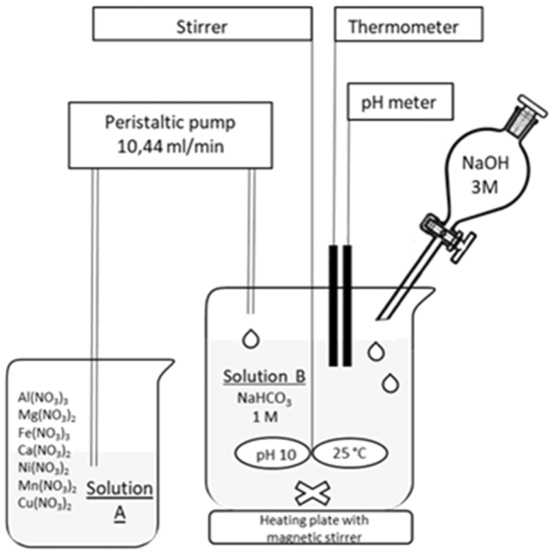

Figure 6. Catalyst preparation scheme.

No correlation was found between the ME content with the pore volume (V_p) and total basicity. This can be explained by the fact that the transesterification occurs on the catalyst surface, because the molecules of TG are bigger than pores. Then, the basic sites inside the pores are inaccessible for the reaction. The ME content was negatively correlated with acidity, a high population of basic sites (high t.a.), and the content of added metal in the EP (X). These three variables were positively correlated with each other. Another positive correlation was between the leaching of magnesium (Mg) and the pore volume, i.e., increasing pore volume caused an increase of magnesium leaching. This can be explained by the fact that leaching of magnesium was caused by methanol, which is presented in pores because it is much smaller than other reaction components. The total basicity was negatively correlated with the aluminum content in the ester phase (Al).

3. CONCLUSIONS

The five different mixed oxides with added divalent metals (Mn, Ca, Co, Ni, and Fe) were used for transesterification of *C. sativa* oil, including detailed statistical analysis of material parameters and transesterification results. The metal cation built into the structure observably influenced the catalytic properties of mixed oxide. Two of the tested mixed oxides demonstrated sufficient catalytic activity. After 7 h of transesterification at 140 °C, the Ni/MO and Fe/MO catalysts reached the methyl ester content higher than 96.5 wt %, which is the minimum prescribed value in the European standard (EN 14214). The lowest amount of leached metal for Ni/MO also indicates that the nickel cation is the most suitable for building into the structure of hydrotalcite/mixed oxide. Next, the research will be focused on reusing this catalyst for better evaluation of its stability. In summary, the catalyst activity increased with the increase of middle basic sites and decreased with acidity and high basic sites, which was also confirmed by statistical analysis. A suitable combination of cations in the heterogeneous catalyst allowed obtaining high methyl ester content after transesterification of *C. sativa* oil.

4. MATERIALS AND METHODS

4.1. Oil Treatment. The camelina oil was obtained by pressing seeds of the variety (L.) Crantz var. Smilowska (CS). The plant was cultivated at The National Agricultural and Food Center in Vígľaš-Pstruša in Slovak Republic. Association Energy 21 in Slovakia realized oil preparation by cold pressing as well as measurements of selected properties (Table 8).

The modified acid degumming method inspired by Sekretár et al.[36] was used to remove unwanted gums such as nonhydratable phospholipids (NHPL) and hydratable phospholipids (HPL) in *C. sativa* (CS). The HPL are readily removable by water, but NHPL must be converted to HPL by acids. In the first step, CS oil was heated to 80 °C with intensive stirring and a solution of citric acid (30 wt %) was added in the amount of 2% (by volume of the oil). After settling at a temperature of 80 °C for 20 min, the oil/acid mixture was cooled down to 25 °C, mixed with water (1%) (by volume of oil), and transferred to a separating funnel. After settling, the solution was drained. To neutralize free fatty acids and remove the soaps, a KOH solution (3 wt %) was added to the oil heated to 80 °C with vigorous stirring. In separating funnels, the soap phase was separated, and oil was washed several times with 10 mL of water until the separated aqueous phase was clear, without soaps, and the pH of the solution was neutral. To remove the water from the oil, the desiccant Na_2SO_4 was added to the oil and heated to 40 °C. After settling at the laboratory temperature, the mixture was filtrated through the Buchner funnel. For the final purification of oil from the residual KOH solution as well as from a desiccant, 5 g of dried clay was added to the oil heated to 40 °C. The treated oil was filtered through a column filled with 50 mL of silica gel placed on a small layer of glass wool. Filtration through silica gel produced a purified oil that was stored in an airtight container in a dark cold place to avoid oxidation. The degumming process removes phospholipids present in raw oil and reduces the metal content in the oil. The phosphorous content decreased below 3 mg/kg, from the original value of more than 13 mg/kg, while the content of other metals (Ca, Mg, etc.) decreased below 1 mg/kg (Table 8).

4.2. Catalyst Preparation. For hydrotalcite (HT) preparation, the coprecipitation method at a constant pH was used (Figure 6). First, the three solutions were prepared: (A) the salt solution (1 mol/dm^3) containing divalent cations (Mn^{2+}, Co^{2+}, Ca^{2+}, Fe^{2+}, Ni^{2+}); (B) $NaHCO_3$ dissolved in deionized water (c = 1 mol/dm^3), and (C) which is a solution of NaOH (3.0 mol/dm^3). Nitrates were used as sources of divalent cations. All materials were prepared at the same conditions: temperature 25 °C and pH 10, which was kept constant by the addition of NaOH solution. The addition of NaOH was controlled by a pH electrode (pHenomenal 1000L, VWR-International GmbH). Solution A was gradually added to solution B at a rate of 4 mL/min and under intensive stirring at 25 °C for 1 h. After preparation, each hydrotalcite was aged without stirring for 24 h. After the suspension sedimentation, the slurry was washed with at least 3 L of distilled water to neutral pH and filtered. Drying was carried out for 1−2 h at 80 °C. After preparation, all HT were calcined in an air atmosphere at a temperature of 450 °C for 4 h to form a mixed oxide structure.

4.3. Catalyst Characterization. The real content of metals in hydrotalcites was determined by the inductively coupled plasma optical emission spectroscopy (ICP-OES)

https://dx.doi.org/10.1021/acsomega.0c04976
ACS Omega 2020, 5, 32040−32050

method. The measurement was performed on the ICP-OES Optima 7000 DV from PerkinElmer. The samples were prepared by dissolving the weighed amount in diluted HCl before measurement. The measurements were carried out using standards adapted to the individual samples of the catalysts based on the metal built into the structure.

The crystalline phase identification of the prepared samples was carried out by XRD analysis using an STOE Theta/Theta diffractometer, with Co Kα radiation, a scan range of 2.90−90.00° 2θ, and at a step size of 0.02°. The XRD of basic hydrotalcite samples dried at 60 °C and of mixed oxides prepared from hydrotalcites by calcination at 450 °C were measured. The lattice parameter (a, c) and basal spacing (d) were determined by the following equation

$$d = \frac{n \cdot \lambda}{2 \sin \theta} \quad (1)$$

where n = 1 and λ = 0.179020 mm.

The crystallite size of the prepared hydrotalcites was calculated using the Scherrer equation

$$D = \frac{K \cdot \lambda}{\beta \cdot \cos \theta} \quad (2)$$

where K = 0.9 and β represents full width at half maximum.[37]

The temperature-dependent weight loss (thermogravimetry) of the HT was measured using a PerkinElmer TGA 4000 thermogravimeter. The measurement was carried out at a temperature range from 30 to 600 °C (10 °C/min) in a nitrogen atmosphere at a pressure of 300 kPa.

The physical adsorption of nitrogen at a temperature of −196 °C using ASAP2400 (Micromeritics) was applied for specific surface measurements. Before the measurements, the samples were degassed under vacuum of 2 Pa at a temperature of 350 °C for one night. Data were evaluated by Brunauer−Emmett−Teller (BET)-isotherm. The micromesoporous characterization was measured using the t-plot. The pore diameter (D_p) was determined by the BJH method.

Acidity was determined by the standard TPD of ammonia in the range of 220−500 °C. Before measurement, the samples (0.3 g) were calcinated at a temperature of 500 °C in helium flow for 2 h and then cooled to 220 °C. Adsorption of ammonia was performed at 220 °C using a mixture of NH_3/He. Desorption of ammonia was carried out from 220 to 700 °C in a flow of helium. The amount of desorbed ammonia represents the overall value of acidity. During desorption, the effluent bubbled through the solution of H_2SO_4 (0.05 M). The amount of unreacted H_2SO_4 was determined by titration with NaOH solution (0.05 M) and served for acidity calculation by the differential method.

The number of basic sites was measured by the standard method, i.e., temperature-programmed desorption of CO_2. The measurement was performed on a Micromeritics AutoChem II 2920 with a Pfeiffer Vacuum OmniStar GSD 320 mass spectrometer. Mixed oxide (100 mg) was placed in a quartz reactor and heated to 500 °C (10 °C/min) in a helium flow at a rate of 25 mL/min. The sample was then cooled to room temperature and saturated in a flow of gas (10 vol % of CO_2 in helium) for 30 min. Afterward, the catalyst was flushed in a flow of helium for 1 h to remove all weakly bound molecules. Desorption of CO_2 was carried out at a linear heating (10 °C/min) in a flow of helium (25 mL/min).[38]

4.4. Transesterification. A nickel−chromium steel (Hastelloy) batch reactor (Parr Instruments, model 4520) was used for the transesterification reaction. The reactor was purged by nitrogen before the reaction. The heterogeneous transesterification in the presence of all prepared mixed oxides was carried out at the same reaction conditions: the molar ratio of methanol to oil was 30:1, there was a 3 wt % of catalyst to oil, the stirring (600 rpm) was done by a shaft stirrer, the constant temperature was at 140 °C, the pressure at 1.05−1.2 MPa, and the reaction time was 7 h. The measurement of the reaction time started when the temperature of the mixture inside the reactor reached 140 °C. Capillary reaching to the bottom of the reactor was installed into the reactor head for samples taken from the reaction mixture during the reaction. The capillary was terminated with a filter to prevent catalyst removal from the reactor. A small amount of the sample for gas chromatography (GC) analysis was taken every hour of the reaction. After sampling, the capillary was purged by a small amount of nitrogen to remove the residues of the product from the capillary. The temperature was held at a constant value with a temperature controller. The mixture of the catalyst, ME, glycerol, and unreacted methanol was obtained after 7 h of reaction. The catalyst was separated by filtration, and methanol was evaporated using a vacuum evaporator. The vessel containing a two-phase mixture of ME and glycerol was placed in the centrifuge to achieve better phase separation. ME and glycerol were weighed after separation and ME was sent to product analysis.

4.5. Product Analysis. The determination of the methyl ester content in products after transesterification was based on the modified standard method EN 14103. The nonadecanoic acid methyl ester was used as the internal standard. Measurement was performed by GC with a flame ionization detector, model Agilent 7890 A series GC, equipped with a split/splitless injector and a programmable oven. As a capillary column, Agilent technologies column BD-EN 14103, with dimensions 30 m × 0.32 mm and a film thickness of 0.25 μm was used. The methyl ester content was calculated according to the standard method EN 14103.

The metal content in the methyl esters was measured by atomic absorption with an iCE 3500 AASpectro Dual Varian EspectrAA-10 plus system (Thermo Scientific). The sample was diluted with xylene and then aspirated into the flame. Absorbances were measured at 589.0 nm.

Methyl ester (ME) yields considering the initial weight of oil were calculated according to the following equation[39]

$$Y\ (\%) = \frac{m_{\text{product}} \cdot x_{\text{ME}}}{m_{\text{oil}}} \quad (3)$$

where m_{product} is the weight of the obtained product (ME plus unconverted acylglycerols) after transesterification, x_{ME} represents the content of ME in the product (wt %), and m_{oil} represents the weight of oil entering the transesterification reaction.

4.6. Statistical Evaluation. The principal component analysis (PCA) was carried out and the component weight plot (CWP) was used to find the relationship between the dependent variables (the program Statistica 12 was used). The explanation of the CWP: variables that are close together have a positive correlation, while variables that are opposite to each other have a negative correlation. If variables are between themselves at right angles, then these variables do not correlate. The variable distance from the center shows how

https://dx.doi.org/10.1021/acsomega.0c04976
ACS Omega 2020, 5, 32040−32050

much the particular variable contributes to individual main components.[39]

■ ASSOCIATED CONTENT

Supporting Information

The Supporting Information is available free of charge at https://pubs.acs.org/doi/10.1021/acsomega.0c04976.

Chromatogram of the total methyl ester content determination in the ester phase after transesterification of *C. sativa* oil according to the modified standard method EN 14103 (Figure S1) (PDF)

■ AUTHOR INFORMATION

Corresponding Author

Elena Hájeková − *Faculty of Chemical and Food Technology, Slovak University of Technology in Bratislava, 812 37 Bratislava, Slovak Republic;* orcid.org/0000-0001-9808-6903; Phone: +421259325404; Email: elena.hajekova@stuba.sk

Authors

Miroslava Mališová − *Faculty of Chemical and Food Technology, Slovak University of Technology in Bratislava, 812 37 Bratislava, Slovak Republic;* orcid.org/0000-0001-5705-6804

Michal Horňáček − *Faculty of Chemical and Food Technology, Slovak University of Technology in Bratislava, 812 37 Bratislava, Slovak Republic;* orcid.org/0000-0001-7363-8775

Jozef Mikulec − *VÚRUP, a.s., 820 03 Bratislava, Slovak Republic*

Pavol Hudec − *Faculty of Chemical and Food Technology, Slovak University of Technology in Bratislava, 812 37 Bratislava, Slovak Republic*

Martin Hájek − *Faculty of Chemical Technology, University of Pardubice, 532 10 Pardubice, Czech Republic*

András Peller − *Faculty of Chemical and Food Technology, Slovak University of Technology in Bratislava, 812 37 Bratislava, Slovak Republic*

Vladimír Jorík − *Faculty of Chemical and Food Technology, Slovak University of Technology in Bratislava, 812 37 Bratislava, Slovak Republic*

Karel Frolich − *Faculty of Chemical Technology, University of Pardubice, 532 10 Pardubice, Czech Republic;* orcid.org/0000-0002-9616-942X

Marcela Hadvinová − *Faculty of Chemical and Food Technology, Slovak University of Technology in Bratislava, 812 37 Bratislava, Slovak Republic;* orcid.org/0000-0002-0511-3130

Complete contact information is available at: https://pubs.acs.org/10.1021/acsomega.0c04976

Author Contributions

This manuscript was written through contributions of all authors. All authors have given approval to the final version of the manuscript. The authors declare that they have no known competing financial interest or personal relationship that could have appeared to influence the work reported in this paper

Notes

The authors declare no competing financial interest.

■ ACKNOWLEDGMENTS

This research has been financially supported by the Slovak Research and Development Agency, grant numbers: APVV-16-0097 and APVV-18-0255 and Czech Science Foundation, Project no. 19-00669S. This work was also supported by the Central European Foundation, Bratislava, as a part of program Talents of New Europe.

■ ABBREVIATIONS

CS	*Camelina sativa*
FAME	fatty acid methyl esters
GC	gas chromatography
HT	hydrotalcite
HPL	hydratable phospholipids
ICP-OES	inductively coupled plasma optical emission spectroscopy
ME	methyl ester
MO	mixed oxides
NHPL	nonhydratable phospholipids
PCA	principal component analysis
TGA	thermogravimetry analysis
TPD-CO_2	temperature-programmed desorption of carbon dioxide
X	added divalent metal
XRD	X-ray diffraction
a	average distance cation−cation, Å
c	thickness of one brucite-like layer and, interlayer, Å
d	basal spacing, Å
D	crystallite size, nm
D_p	pore diameter, nm
$m_{product}$	weight of product (ME + unreacted oil), g
m_{oil}	weight of oil, g
S_{BET}	specific surface area, m^2/g
TWL	total weight losses, wt %
V_p	pore volume, cm^3/g
WL	weight losses, wt %
x_{ME}	content of ME in product, wt %
Y	methyl ester yield, %

■ REFERENCES

(1) Knothe, G. Biodiesel and Renewable Diesel: A Comparison. *Prog. Energy Combust. Sci.* **2010**, *36*, 364−373.

(2) Zubr, J. Oil-Seed Crop: *Camelina sativa*. *Ind. Crops Prod.* **1997**, *6*, 113−119.

(3) Hrastar, R.; Petrišič, M. G.; Ogrinc, N.; Košir, I. J. Fatty Acid and Stable Carbon Isotope Characterization of *Camelina sativa* Oil: Implications for Authentication. *J. Agric. Food Chem.* **2009**, *57*, 579−585.

(4) Hoekman, S. K.; Broch, A.; Robbins, C.; Ceniceros, E.; Natarajan, M. Review of Biodiesel Composition, Properties, and Specifications. *Renewable Sustainable Energy Rev.* **2012**, *16*, 143−169.

(5) Schuchardt, U.; Sercheli, R.; Vargas, R. M. Transesterification of Vegetable Oils: A Review. *J. Braz. Chem. Soc.* **1998**, *9*, 199−210.

(6) Meher, L. C.; Vidya Sagar, D.; Naik, S. N. Technical Aspects of Biodiesel Production by Transesterification - A Review. *Renewable Sustainable Energy Rev.* **2006**, *10*, 248−268.

(7) Endalew, A. K.; Kiros, Y.; Zanzi, R. Inorganic Heterogeneous Catalysts for Biodiesel Production from Vegetable Oils. *Biomass Bioenergy* **2011**, *35*, 3787−3809.

(8) Semwal, S.; Arora, A. K.; Badoni, R. P.; Tuli, D. K. Biodiesel Production Using Heterogeneous Catalysts. *Bioresour. Technol.* **2011**, *102*, 2151−2161.

(9) Dossin, T. F.; Reyniers, M. F.; Berger, R. J.; Marin, G. B. Simulation of Heterogeneously MgO-Catalyzed Transesterification

for Fine-Chemical and Biodiesel Industrial Production. *Appl. Catal., B* **2006**, *67*, 136−148.
(10) Zhang, Y.; Dubé, M. A.; McLean, D. D.; Kates, M. Biodiesel Production from Waste Cooking Oil: 1. Process Design and Technological Assessment. *Bioresour. Technol.* **2003**, 1−16.
(11) Nishimura, S.; Takagaki, A.; Ebitani, K. Characterization, Synthesis and Catalysis of Hydrotalcite-Related Materials for Highly Efficient Materials Transformations. *Green Chem.* **2013**, *15*, 2026−2042.
(12) Arruda, C. C.; Cardoso, P. H. L.; Dias, I. M. M.; Salomão, R. Hydrotalcite (Mg 6 Al 2 (OH) 16 (CO 3)·4H 2 O): A Potentially Useful Raw Material for Refractories. *Interceram* **2013**, *62*, 187−191.
(13) Luggren, P. J.; Apesteguía, C. R.; di Cosimo, J. I. Upgrading of Biomass-Derived 2-Hexanol to Liquid Transportation Fuels on Cu-Mg-Al Mixed Oxides. Effect of Cu Content. *Fuel* **2016**, *177*, 28−38.
(14) Daza, C. E.; Gallego, J.; Mondragón, F.; Moreno, S.; Molina, R. High Stability of Ce-Promoted Ni/Mg-Al Catalysts Derived from Hydrotalcites in Dry Reforming of Methane. *Fuel* **2010**, *89*, 592−603.
(15) Kou, J. W.; Cheng, S. Y.; Bai, J. L. Effects of Amino Trimethylene Phosphonic Acid on Structure and Properties of Cu−Zn−Al Hydrotalcite-Derived Oxides for Catalytic Synthesis of Iso-Butanol and Ethanol from Synthesis Gas. *Fuel* **2019**, *255*, No. 115833.
(16) Wang, S. H.; Wang, Y. B.; Dai, Y. M.; Jehng, J. M. Preparation and Characterization of Hydrotalcite-like Compounds Containing Transition Metal as a Solid Base Catalyst for the Transesterification. *Appl. Catal., A* **2012**, *439*−*440*, 135−141.
(17) Wang, Y.-B.; Jehng, J. M. Hydrotalcite-like Compounds Containing Transition Metals as Solid Base Catalysts for Transesterification. *Chem. Eng. J.* **2011**, *175*, 548−554.
(18) Man, L. F.; Wong, W. T.; Yung, K. F. Alkali Hydrothermal Synthesis of Na 0.1Ca 0.9TiO 3 Nanorods as Heterogeneous Catalyst for Transesterification of *Camelina sativa* Oil to Biodiesel. *J. Cluster Sci.* **2012**, *23*, 873−884.
(19) Patil, P. D.; Deng, S. Transesterification of *Camelina sativa* Oil Using Heterogeneous Metal Oxide Catalysts. *Energy Fuels* **2009**, *23*, 4619−4624.
(20) Perea, A.; Kelly, T.; Hangun-Balkir, Y. Utilization of Waste Seashells and *Camelina sativa* Oil for Biodiesel Synthesis. *Green Chem. Lett. Rev.* **2016**, *9*, 27−32.
(21) Navajas, A.; Campo, I.; Moral, A.; Echave, J.; Sanz, O.; Montes, M.; Odriozola, J. A.; Arzamendi, G.; Gandía, L. M. Outstanding Performance of Rehydrated Mg-Al Hydrotalcites as Heterogeneous Methanolysis Catalysts for the Synthesis of Biodiesel. *Fuel* **2018**, *211*, 173−181.
(22) Silva, C. C. C. M.; Ribeiro, N. F. P.; Souza, M. M. V. M.; Aranda, D. A. G. Biodiesel Production from Soybean Oil and Methanol Using Hydrotalcites as Catalyst. *Fuel Process. Technol.* **2010**, *91*, 205−210.
(23) Cantrell, D. G.; Gillie, L. J.; Lee, A. F.; Wilson, K. Structure-Reactivity Correlations in MgAl Hydrotalcite Catalysts for Biodiesel Synthesis. *Appl. Catal., A* **2005**, *287*, 183−190.
(24) Hernández, W. Y.; Aliç, F.; Verberckmoes, A.; van der Voort, P. Tuning the Acidic−Basic Properties by Zn-Substitution in Mg−Al Hydrotalcites as Optimal Catalysts for the Aldol Condensation Reaction. *J. Mater. Sci.* **2017**, *52*, 628−642.
(25) Wei, Q.; Gao, X.; Liu, G.; Yang, R.; Zhang, H.; Yang, G.; Yoneyama, Y.; Tsubaki, N. Facile One-Step Synthesis of Mesoporous Ni-Mg-Al Catalyst for Syngas Production Using Coupled Methane Reforming Process. *Fuel* **2018**, *211*, 1−10.
(26) Jiang, Z.; Yu, J.; Cheng, J.; Xiao, T.; Jones, M. O.; Hao, Z.; Edwards, P. P. Catalytic Combustion of Methane over Mixed Oxides Derived from Co-Mg/Al Ternary Hydrotalcites. *Fuel Process. Technol.* **2010**, *91*, 97−102.
(27) Castro, C. S.; Garcia, L. C. F.; Assaf, J. M. The Enhanced Activity of Ca/MgAl Mixed Oxide for Transesterification. *Fuel Process. Technol.* **2014**, *125*, 73−78.
(28) Martins, M. I.; Pires, R. F.; Alves, M. J.; Hori, C. E.; Reis, M. H. M.; Cardoso, V. L. Transesterification of Soybean Oil for Biodiesel Production Hydrotalcite as Basic Catalyst. *Chem. Eng. Trans.* **2013**, *32*, 817−822.
(29) di Serio, M.; Ledda, M.; Cozzolino, M.; Minutillo, G.; Tesser, R.; Santacesaria, E. Transesterification of Soybean Oil to Biodiesel by Using Heterogeneous Basic Catalysts. *Ind. Eng. Chem. Res.* **2006**, *45*, 3009−3014.
(30) Macala, G. S.; Robertson, A. W.; Johnson, C. L.; Day, Z. B.; Lewis, R. S.; White, M. G.; Iretskii, A. V.; Ford, P. C. Trans-esterification Catalysts from Iron Doped Hydrotalcite-like Precursors: Solid Bases for Biodiesel Production. *Catal. Lett.* **2008**, *122*, 205−209.
(31) Zaleckas, E.; Makareviciene, V.; Sendžikiene, E. Possibilities of Using *Camelina sativa* Oil for Producing Biodiesel Fuel. *Transport* **2012**, *27*, 60−66.
(32) Mootabadi, H.; Salamatinia, B.; Bhatia, S.; Abdullah, A. Z. Ultrasonic-Assisted Biodiesel Production Process from Palm Oil Using Alkaline Earth Metal Oxides as the Heterogeneous Catalysts. *Fuel* **2010**, *89*, 1818−1825.
(33) Bancquart, S.; Vanhove, C.; Pouilloux, Y.; Barrault, J. Glycerol Transesterification with Methyl Stearate over Solid Basic Catalysts I. Relationship between Activity and Basicity. *Appl. Catal., A* **2001**, *218*, 1−11.
(34) Yan, S.; Salley, S. O.; Simon Ng, K. Y. Simultaneous Transesterification and Esterification of Unrefined or Waste Oils over ZnO-La2O3 Catalysts. *Appl. Catal., A* **2009**, *353*, 203−212.
(35) Lee, Hv.; Juan, J. C.; Taufiq-Yap, Y. H.; Kong, P. S.; Rahman, N. A. Advancement in Heterogeneous Base Catalyzed Technology: An Efficient Production of Biodiesel Fuels. *J. Renewable Sustainable Energy* **2015**, *7*, No. 032701.
(36) Sekretár, S.; Zufarov, O.; Schmidt, Š. Degumming of Rapeseed and Sunflower Oils. *Acta Chim. Slov.* **2008**, *1*, 321−328.
(37) Frolich, K.; Vávra, A.; Kocík, J.; Hájek, M.; Jílková, A. The Long-Term Catalytic Performance of Mixed Oxides in Fixed-Bed Reactors in Transesterification. *Renewable Energy* **2019**, *143*, 1259−1267.
(38) Hájek, M.; Skopal, F.; Vávra, A.; Kocík, J. Transesterification of Rapeseed Oil by Butanol and Separation of Butyl Ester. *J. Cleaner Prod.* **2017**, *155*, 28−33.
(39) Bartholomew, D. J. Principal Components Analysis. *Encyclopedia of Education*; Elsevier Ltd.: London, U.K., 2010; pp 374−377.

https://dx.doi.org/10.1021/acsomega.0c04976
ACS Omega 2020, 5, 32040−32050